CHAPTER 6 - COMPARATIVE ANALYSIS OF MECHANICAL CONSOLIDATION AND ELECTROKINETIC CONSOLIDATION

6.1 General

This chapter discusses a detailed design outline of continuous controlled-strain and controlled-stress axial compression for expediting the consolidation process named electrokinetic consolidometer and the procedure involved with the sample preparation and compared with the data obtained from conventional IL, CL and CRS consolidation tests. But in the case of electrokinetic consolidation, no such standard code of practice is available. To carry out the test, an existing consolidation cell was modified and fabricated indigenously as per the ASTM standard protocols mentioned with a D/H ratio equivalent to 2.5. Some of the critical considerations for the setup required for the electro-osmosis test are (i) easy provision for early dissipation of generated pore water pressure and early expulsion of developed gases; (ii) continuous automated data monitoring in real-time with Data Acquisition System (DAQ) at regular time intervals without interruption; (iii) availability and suitability of sensor with DAQ for multiple parameter measurements such as deformation, current, and voltage measurement with time.

6.2. EK Experimental Programme

Table 6.1 summarizes the consolidation tests performed on geomaterials (marine soil, black cotton soil, and red mud) with and without the application of an electric gradient. Test results are reported in Table 6.2 with regard to Marine soil and black cotton soils. In this study, pore water pressure was not generated sufficiently during consolidation tests performed with EK coupled incremental loading (EKIL) up to 4.0 kg/cm^2, and EKCL tests at small loadings such as 0.25, 0.50, and 1.0 kg/cm^2 during the initial stages of the

experiment. The EKCRS tests conducted at a low strain rates coupled with constant voltage did not generate enough data due to insufficient pore pressure conditions.

Table 6.1 Details of the laboratory experimental programme

Testing Parameters / Test Combination	σ_v, max at end (kg/cm^2)	Strain rate (mm/min)	Strain rate (%/min)	ΔΦ (V_0)	ΔΦ/L (V/cm)
IL loading tests with conventional and modified consolidation cell					
ILMS-C	Upto 4.0	-	-	-	-
ILMS-M	Upto 4.0	-	-	-	-
ILBCS-C	Upto 4.0	-	-	-	-
ILBCS-M	Upto 4.0	-	-	-	-
ILRM-M	Upto 4.0	-	-		
Using modified consolidation cell					
CLMS-M	4.0	-	-	-	-
EKCLMS1	4.0	-	-	2	0.5
EKCLMS2	4.0	-	-	4	1.0
EKCLMS3	4.0	-	-	6	1.5
CRSMS1	8.0	0.002	0.005	-	-
CRSMS4	8.0	0.005	0.0125	-	-
EKCRSMS1	4.0	0.005	0.0125	2	0.5
EKCRSMS2	4.0	0.005	0.0125	4	1.0
EKCRSMS3	4.0	0.005	0.0125	6	1.5
CLBCS-M	4.0	-	-	-	-
EKCLBCS1	4.0	-	-	2	0.5
EKCLBCS2	4.0	-	-	4	1.0
EKCLBCS3	4.0	-	-	6	1.5
CRSBCS1	8.0	0.0025	0.00625	-	-
CRSBCS4	8.0	0.0075	0.01875	-	-
EKCRSBCS1	4.0	0.0075	0.01875	2	0.5
EKCRSBCS2	4.0	0.0075	0.01875	4	1.0
EKCRSBCS3	4.0	0.0075	0.01875	6	1.5
CRSRM1	8.0	0.1	0.25	-	-
CRSRM4	8.0	0.5	1.25	-	-
CRSRM2	-	0.125	0.3125	-	
EKCLRM2	4.0	-		4	1.0

The electrokinetic (EK) technique was found to be more promising for the early dissipation of pore pressure even at high strain rates and achieving maximum settlement by reducing the overall time duration. Furthermore, additional parameters were examined based on pre and post-test results for various loading conditions and are provided in Tables 6.2 and 6.3

Table 6.2 Experimental results of conventional IL, CL and EKCL consolidation methods

Loading condition → / Parameters ↓	Soil type	EKCLMS1/ EKCLBCS1	EKCLMS2/ EKCLBCS2	EKCLMS3/ EKCLBCS3	ILMS-M/ ILBCS-M	CLMS-M/ CLBCS-M	ILMS-C/ ILBCS-C
Consolidation ring type		**Modified consolidation ring**					**Conventional consolidation ring**
Max. settlement after loading (mm)	MS	12.121	12.36*	12.298	9.923	9.286	6.012
	BCS	10.045	10.916	10.526	8.181	7.437	5.064
Final settlement after unloading (mm)	MS	11.376	11.873*	11.64	8.53	7.844	5.018
	BCS	9.324	10.412	10.048	7.068	6.316	4.182
Time to reach final settlement (hrs.)	MS	52.5	84.9	31.94*	144.6	114.27	144.6
	BCS	40.33	54.68	47.167	144.6	105.67	144.6
50% Settlement value after loading	MS	6.11	6.216	6.211	4.964	4.698	3.006
	BCS	5.023	5.458	5.263	4.091	3.718	2.532
Time to reach 50% settlement (hrs.)	MS	0.534	0.817	0.567	75.334	0.379	74.678
	BCS	0.517	0.8	0.783	74.317	0.363	74.332
90% Settlement value after loading	MS	10.914	11.126	11.079	8.948	8.366	5.411
	BCS	9.041	9.818	9.473	7.363	6.693	4.558
Time to reach 90% settlement (hrs.)	MS	4.55	6.98	3.56	120.5	2.652	123.056
	BCS	6.523	6.812	5.962	116.32	2.562	119.526

Table 6.2 Continued.

Percentage regains (%)	MS	6.550	4.102*	5.653	16.33	18.38	19.808
	BCS	7.732	4.840	4.957	15.740	17.750	21.090
Initial void ratio	MS	1.649	1.626*	1.648	1.624	1.631	1.738
	BCS	1.096	1.106	1.098	1.104	1.10	1.112
Final void ratio	MS	0.846	0.828*	0.834	0.983	1.02	0.99
	BCS	0.558	0.548	0.554	0.632	0.674	0.612
Coefficient of volume change (per kPa)	MS	$7.57x10^{-4}$	$7.73x10^{-4}$	$7.69x10^{-4}$	$5.32x10^{-4}$	$5.8x10^{-4}$	$4.94x10^{-4}$
	BCS	$6.41x10^{-4}$	$6.624x10^{-4}$	$6.482x10^{-4}$	$5.608x10^{-4}$	$5.071x10^{-4}$	$4.62x10^{-4}$
Coefficient of consolidation-c_v (mm^2/sec)	MS	$2.81x10^{-2}$	$2.99\ x10^{-2}$	$3.13\ x10^{-2}$	$1.87\ x10^{-2}$	$1.35\ x10^{-2}$	$6.46\ x10^{-2}$
	BCS	$4.62x10^{-2}$	$4.89\ x10^{-2}$	$5.23\ x10^{-2}$	$2.01\ x10^{-2}$	$1.77\ x10^{-2}$	$5.52\ x10^{-2}$
Current (mA)	MS	118.71	163.14	322.08	--	--	--
	BCS	119.63	198.23	322.943	--	--	--
Energy consumption (Wh)	MS	12.47	55.41	61.72	--	--	--
	BCS	9.649	43.356	91.393	--	--	--

Table 6.3 Test results of EKCRS and CRS techniques using modified consolidation ring

Loading condition → / Parameters ↓	Soil Type	EKCRSMS1/ EKCRSBCS1	EKCRSMS2/ EKCRSBCS2	EKCRSMS3/ EKCRSBCS3	CRSMS1/ CRSBCS1	CRSMS4/ CRSBCS4
Maximum deformation (mm)	MS	12.598	13.213	13.811	13.594	11.838
	BCS	10.42	11.234	11.396	11418	10.105
Increase in deformation reference to CRS4 (mm)	MS	0.760	1.375	1.973	1.756	Reference
	BCS	0.318	1.129	1.291	1.313	Reference
Deformation after unloading (mm)	MS	10.908	10.985	11.185	10.085	9.341
	BCS	8.908	9.348	9.414	8.506	8.123
Change in deformation (mm)	MS	1.69	2.228	2.626	3.509	2.497
	BCS	0.512	1.886	1.982	3.112	2.212
Time to reach maximum deformation (hrs.)	MS	43.98	45.16	46.33	119.33	41.08
	BCS	22.734	23.567	24.66	71.83	23.383
Post-Pore Pressure ratio (PPR)	MS	0.015	0.125	0.34	0.083	0.263
	BCS	---	---	---	---	---

Table 6.3 Continued.

End pore pressure value (kg/cm^2)	MS	0.272	0.40	1.76	0.58	1.22
	BCS	--	--	--	--	--
Initial void ratio	MS	1.649	1.626	1.648	1.738	1.758
	BCS	1.106	1.104	1.11	1.106	1.11
Final void ratio	MS	0.846	0.8279	0.834	0.817	0.94
	BCS	0.542	0.55	0.566	0.522	0.53
Coefficient of volume change (per kPa)	MS	6.12×10^{-4}	6.33×10^{-4}	6.38×10^{-4}	3.4×10^{-4}	5.23×10^{-4}
	BCS	7.38×10^{-4}	7.65×10^{-4}	7.81×10^{-4}	4.67×10^{-4}	6.54×10^{-4}
Coefficient of consolidation-c_v (mm^2/sec)	MS	3.91×10^{-2}	4.29×10^{-2}	5.01×10^{-2}	1.87×10^{-2}	3.35×10^{-2}
	BCS	4.61×10^{-2}	4.98×10^{-2}	5.33×10^{-2}	2.31×10^{-2}	4.21×10^{-2}
Current (mA)	MS	93.990	142.810	318.530	--	--
	BCS	112.850	121.823	353.663	--	--
Energy consumption (Wh)	MS	8.14	25.42	43.96	--	--
	BCS	5.131	11.484	52.327	--	--

In summary, this study investigated the use of an electric gradient to improve consolidation in marine soil and black cotton soil. The results suggest that EK is a promising technique for early pore pressure dissipation and achieving maximum settlement. However, more research is needed to further understand the mechanisms involved and optimize the parameters for different loading conditions.

6.2.1 Axial deformation vs time

Figures 6.1(a), (b), (c), (d) and (e) display the results of experiments that examined deformation of marine soils, black cotton soil and red mud under different loading conditions. During the experiments, a linear variable differential transducer (LVDT) was placed at the top of the loading pad to record deformation data continuously using DAQ. The settlement for EK coupled loadings (EKCL and EKCRS) was observed to be higher than that of conventional mechanical loading (IL, CL, and CRS) consolidation process. This additional deformation occurs due to the electro-osmotic flow process, which dissipates excess pore water generated due to the voltage gradient in EKCL and EKCRS.

This phenomenon involves the transport of ions under an electric gradient, including diffusion, electromigration, and electro-osmotic flux advection, which leads to faster dissipation of excess pore water, altering the soil fabric due to pore fluid flow, ion migration, and charged particle flow. The electro-osmotic flow is directly proportional to the applied electric potential. The maximum settlement occurred when the voltage gradient was equal to unity for EKCL loading, while for EKCRS loading condition, a maximum deformation occurred for 1.5 voltage gradient. The unloading trend was favorable for the voltage gradient equal to unity, making it more suitable for application. Figures 6.1(a), (b),

(c), (d) and (e) show the axial deformation vs time trend for marine soil, black cotton soil, and red mud for different loading conditions.

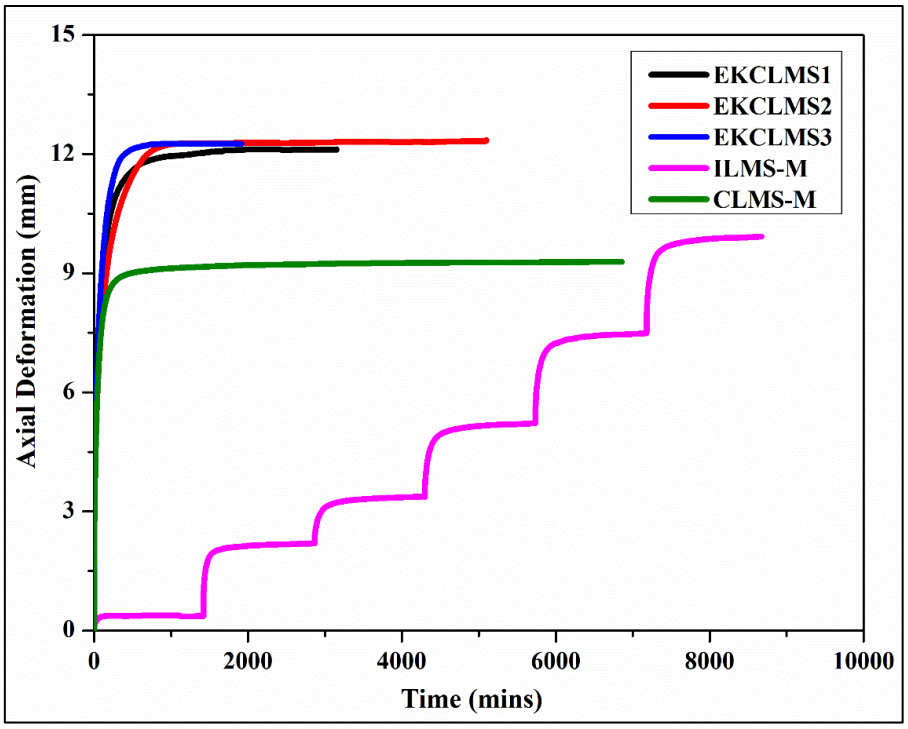

(a)

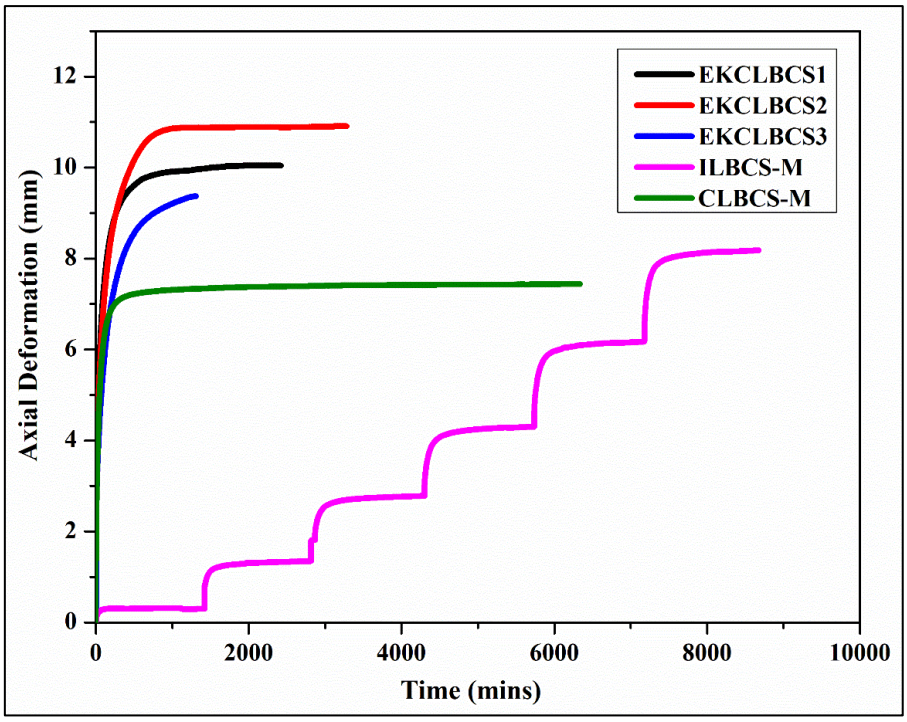

(b)

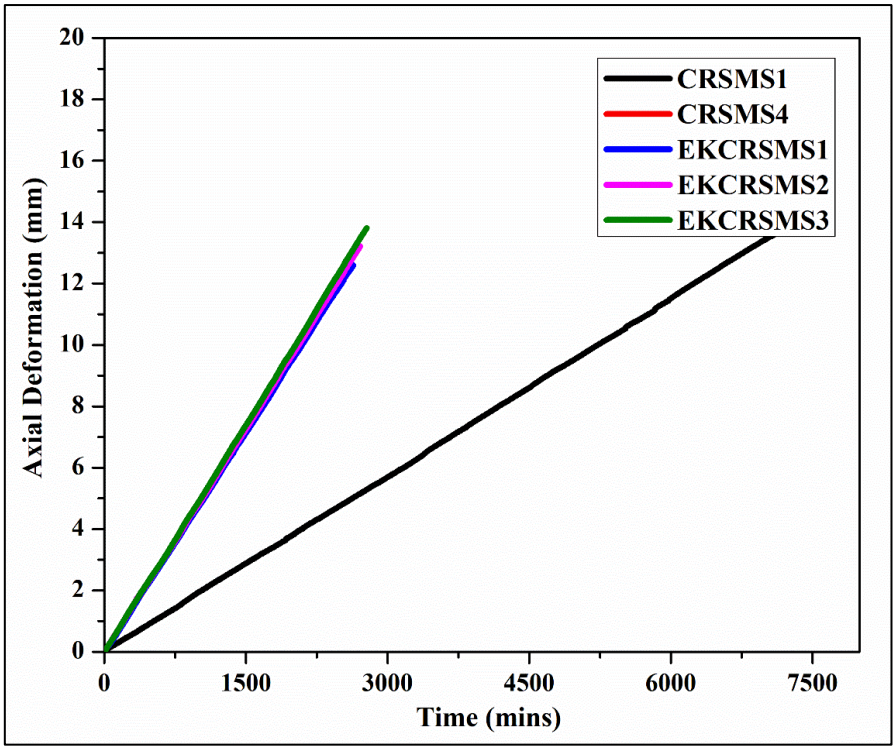
CRSMS1
CRSMS4
EKCRSMS1
EKCRSMS2
EKCRSMS3
Axial Deformation (mm)
Time (mins)
0
2
4
6
8
10
12
14
16
18
20
0
1500
3000
4500
6000
7500

(c)

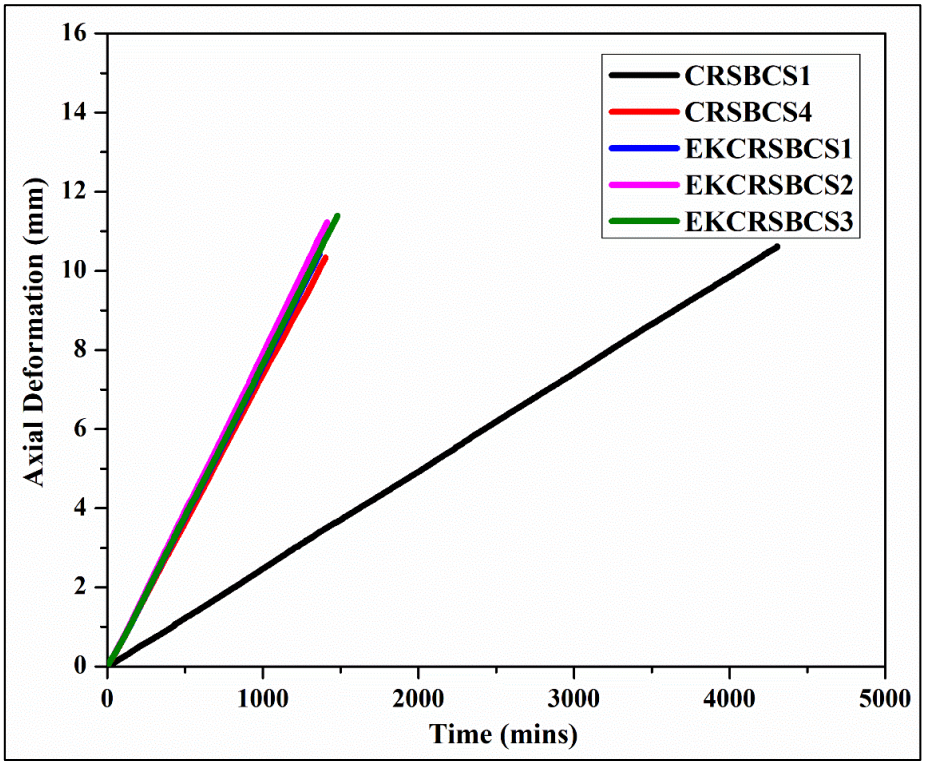
CRSBCS1
CRSBCS4
EKCRSBCS1
EKCRSBCS2
EKCRSBCS3
Axial Deformation (mm)
Time (mins)
0
2
4
6
8
10
12
14
16
0
1000
2000
3000
4000
5000

(d)

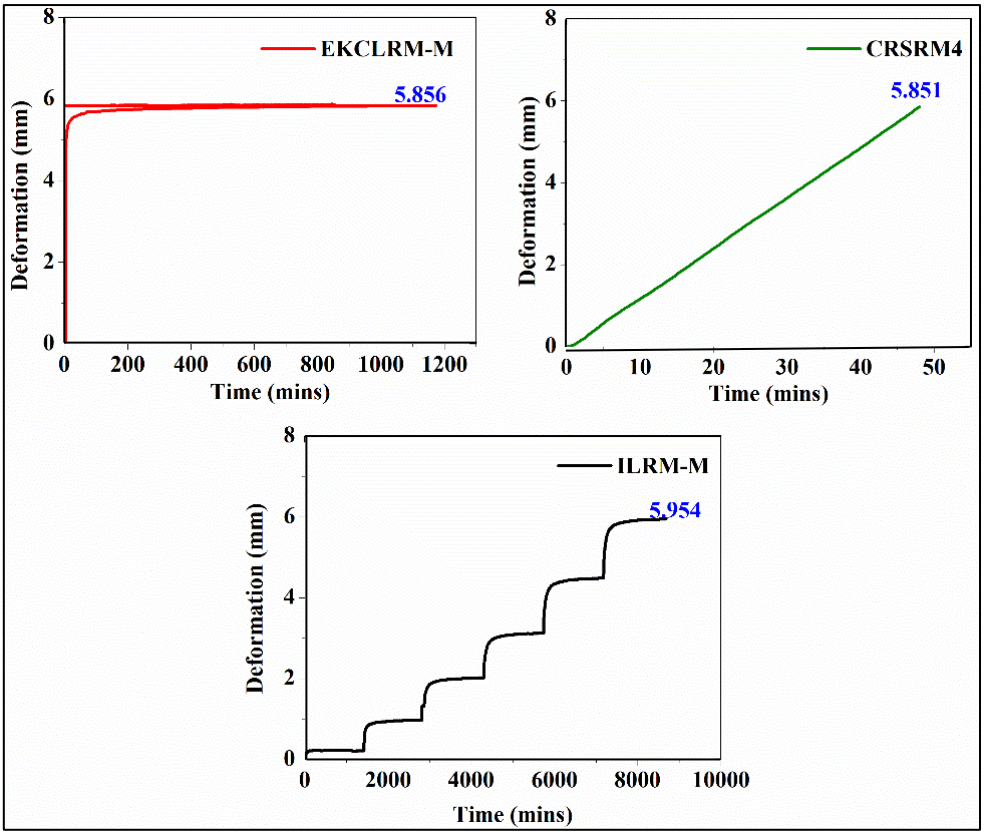

(e.)

Figure 6.1 The axial deformation trend with time of two different loading combinations; (i) IL-M, CL-M, and EKCL loading for (a) Marine soil and (b) Black cotton soil; (ii) CRS, and EKCRS loading for (c) Marine soil and (d) Black cotton soil and (iii) IL-M, CRS, EKCL loading (e) Red mud

The test results of EK coupled consolidation with a modified consolidometer ring for marine soil showed an additional settlement of 2.198 mm, 2.437 mm, and 2.375 mm when the DC voltages of 2V, 4V, and 6V respectively, were coupled with the incremental load of 4kg/cm^2. This was in comparison to the settlement observed at a constant loading of 4 kg/cm^2. Similarly, for black cotton soil, an additional settlement of 1.864 mm, 2.735 mm, and 2.345 mm was observed for the same conditions. Figure 6.2(a) and (b) shows the deformation trends for different loading condition for marine soil and black cotton soil.

For the 0.005 mm/min strain rate coupled loading, an additional settlement of 0.760 mm, 1.375 mm, and 1.973 mm was observed with DC voltages of 2V, 4V, and 6V, respectively, compared to the settlement value observed in constant strain loading of 0.005 mm/min

applied without DC voltage. For the 0.0075 mm/min strain rate coupled loading, an additional settlement of 0.315 mm, 1.129 mm, and 1.291 mm was observed with DC voltages of 2V, 4V, and 6V, respectively, compared to the settlement value observed in constant strain loading of 0.0075 mm/min applied without DC voltage. The coupled EK test was completed in less time than the traditional consolidation tests with a modified oedometer.

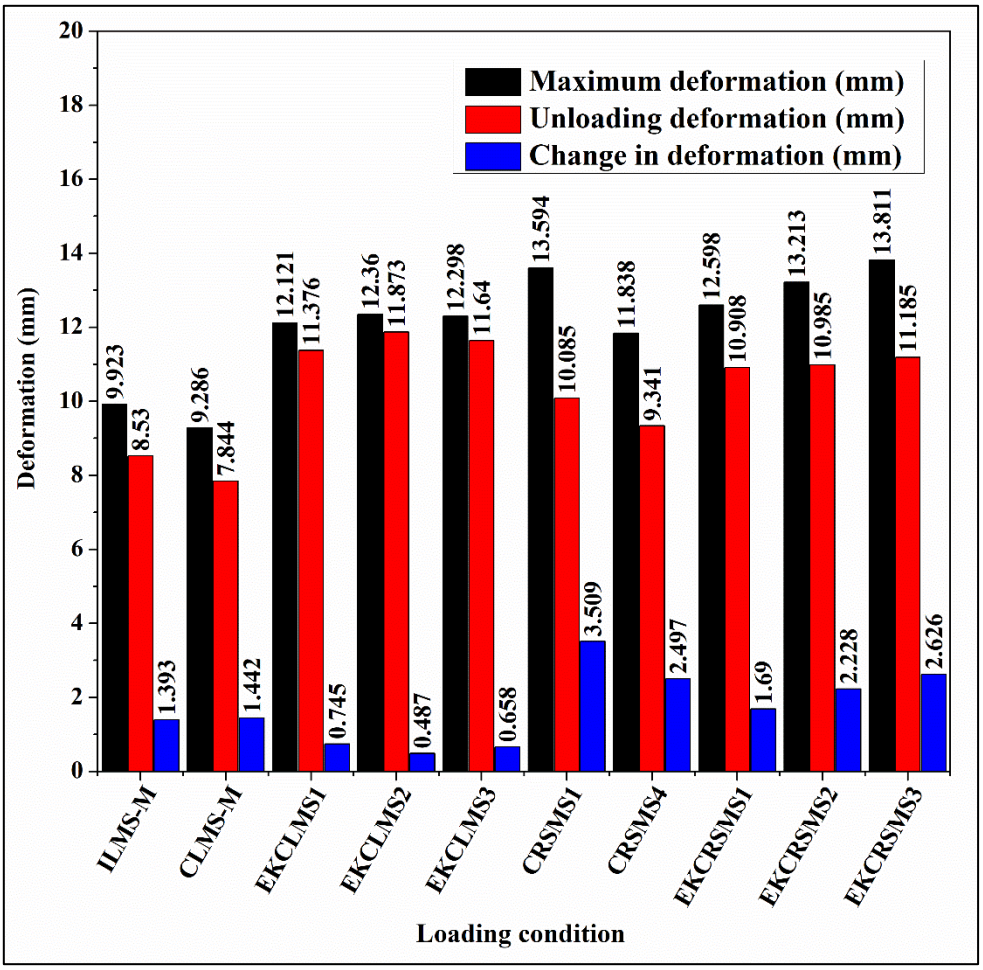

(a)

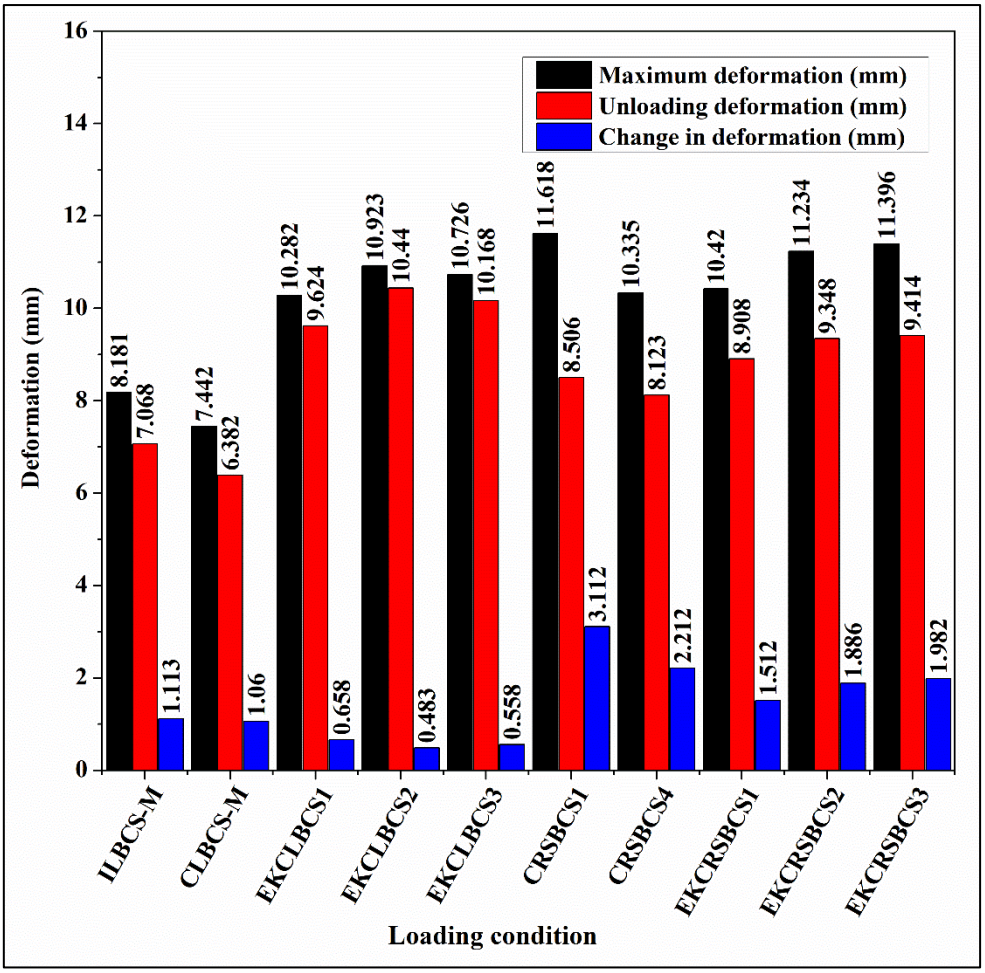

(b)

Figure 6.2 Axial deformation and corresponding time for different loading conditions using modified consolidation ring for (a) Marine soil and (b) Black cotton soil

6.2.2 Void ratio vs time

Figure 6.3(a) and (b) depicts the change in void ratio over time for different loading conditions. At the beginning of the test, an increase in negative excess pore pressure develops from the top (cathode) to the bottom (anode), which elevates the effective stress in the soil. As a result, the void ratio decreases over time due to the additional expulsion of pore water, particularly in the case of EKCL and EKCRS coupled loading. Consequently, the faster dissipation of excess pore water pressure due to a combined electro-mechanical loading system for a given voltage gradient leads to more compression and additional settlement compared to mechanical loading alone. This finding has also been reported in other studies (Jeyakanthan et al., 2011; Huey 2016; Malekzadeh and Sivakugan 2017;

Gingine and Cardoso 2017). Moreover, based on previous research, an EKCL test generates the most compression and a corresponding decrease in void ratio for a voltage gradient of 1V/cm. Similar trends were observed for EKCL and EKCRS, which are equivalent to a voltage gradient of 1V/cm.

Furthermore, it was noted that the maximum final settlement value for a given time was greater for 6V DC than for 2V and 4V DC coupled with constant loading in marine soil. Table 6.2 presents the test results for settlement and void ratio due to voltage coupled loading and mechanical loading. In summary, Figure 6.3 provides valuable insights into the behavior of soil under different loading conditions, emphasizing the impact of electro-mechanical coupling on soil deformation and settlement.

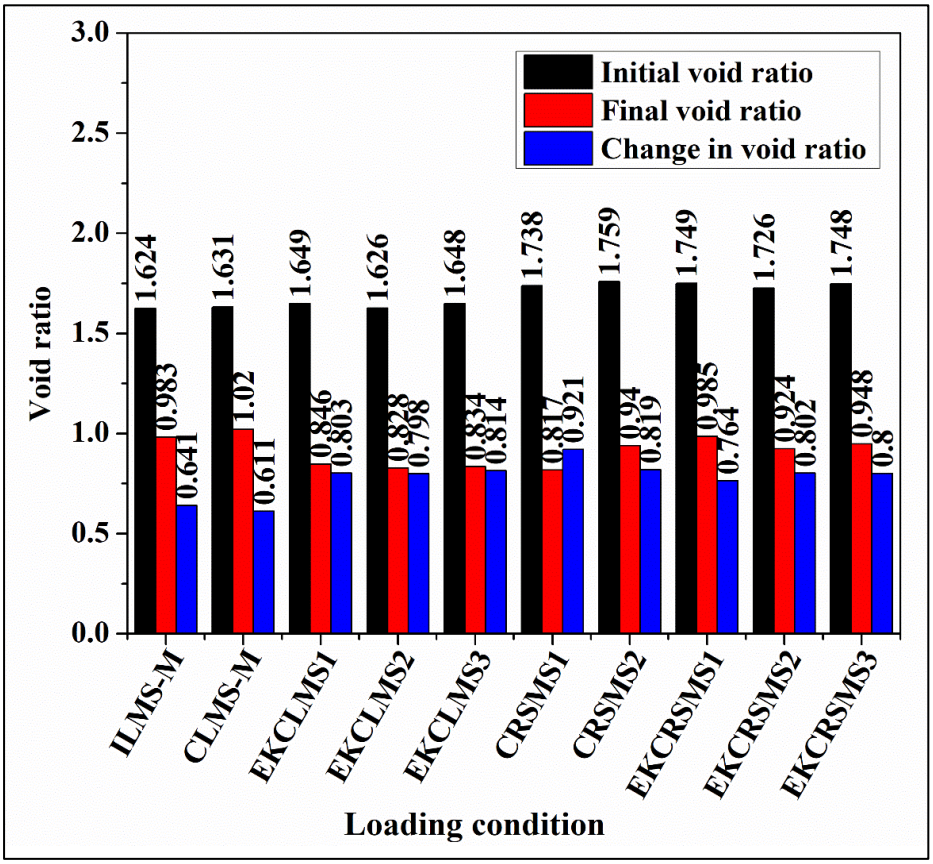

(a)

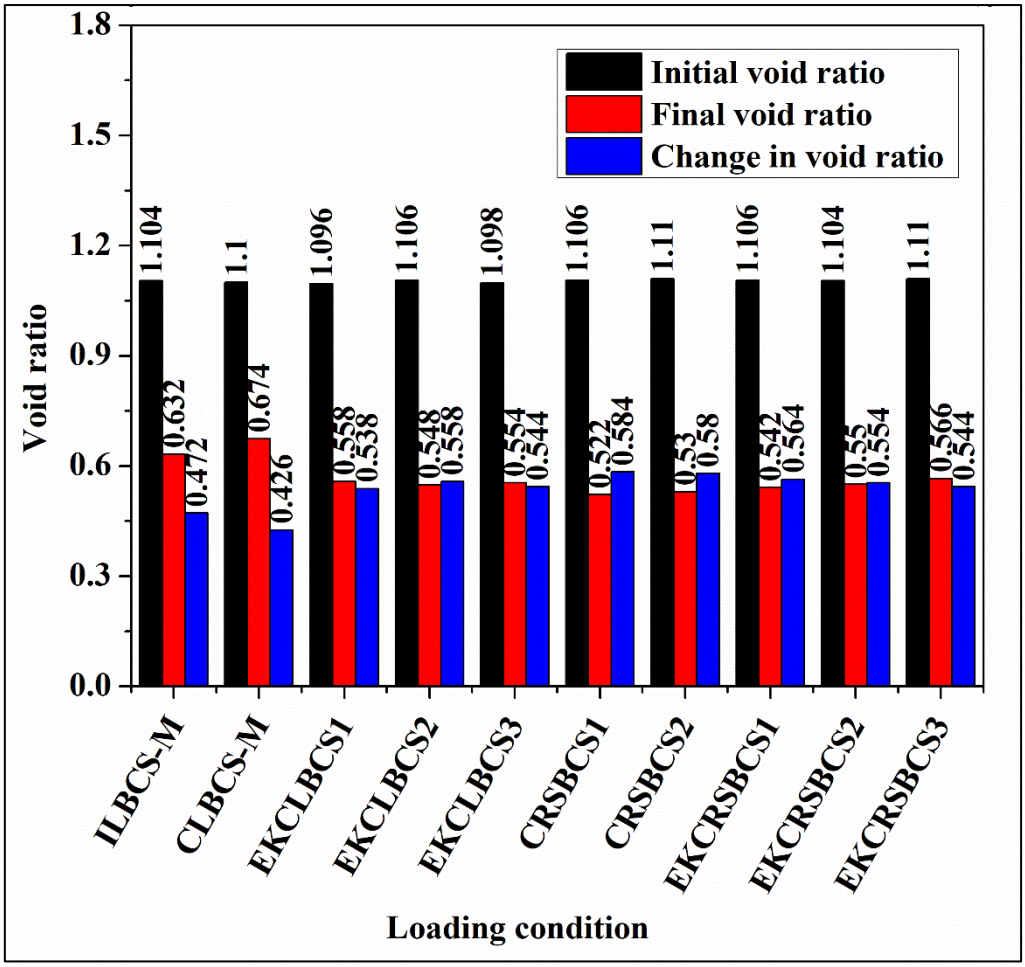

(b)

Figure 6.3 Void ratio vs loading condition for trend for different loading conditions using modified consolidation ring for (a) Marine soil and (b) Black cotton soil.

6.2.3 Pore pressure vs Time

Figure 6.4 illustrates the variation of pore pressure with time for CRSMS1 and CRSMS4 (0.002 and 0.005 mm/min) and with EKCRSMS1, EKCRSMS2 and EKCRSMS3 in the modified consolidometer ring. To measure the continuous pore pressure data during automated loading, a pore pressure transducer is placed at the bottom of the consolidation setup and connected with DAQ. In the case of a constant rate of strain loading, the pore pressure value increased with increase in axial loading intensity. Whereas, in case of EKCRS loading, pore pressure observed during the application of voltage gradients of 2, 4 and 6V coupled with 0.005 mm/min showed a similar trend as observed in constant rate of strain loading. For 2V coupled constant rate of strain loading condition, an insignificant

generation of pore pressure in the soil was noticed. Whereas, in case of 4 and 6V coupled constant rate of strain loadings, negative pore pressure was observed due to the generation of a significant amount of gas because of electrochemical reaction during the initial stage of the test. Later on, upon reaching a substantial amount of load, the gas expulsion occurred, and the negative pore water pressure value changed to positive.

6.2.4 Pore pressure ratio (PPR) vs Time

Figure 6.5 illustrates the variation of pore pressure ratio (u_b/σ_b) with time for CRSMS1 and CRSMS4 (0.002 and 0.005 mm/min) and with EKCRSMS1, EKCRSMS2 and EKCRSMS3 tests performed using the modified consolidometer. In CRS loading, the PPR is dependent on the generated pore pressure and applied total stress, and with an increase in total stress, the PPR shows an increasing trend due to the dissipation of pore water from the voids of the sample. In EKCRS loading, with an increase in time and total stress, a similar trend of the PPR value is observed to some extent. In case of electrokinetic constant-rate-of-strain, lower values of PPR were noticed than the PPR values observed in constant rate of strain loading at 0.005 mm/min. This decrease in PPR value was due to the early pore pressure dissipation because of occurrence of electro-osmosis in the presence of DC voltage. In case of high DC voltages 4 and 6V coupled with high strain rate for constant rate of strain loading tests, both positive and negative values have been found due to negative and positive pore pressure ratio values. The criteria to meet the pore pressure ratio values range between 0.03-0.15 was found to be satisfied in case of EKCRS2 coupled loading while the same was observed only in case of low strain constant rate of strain loading rate with increased test duration at 0.002 mm/min.

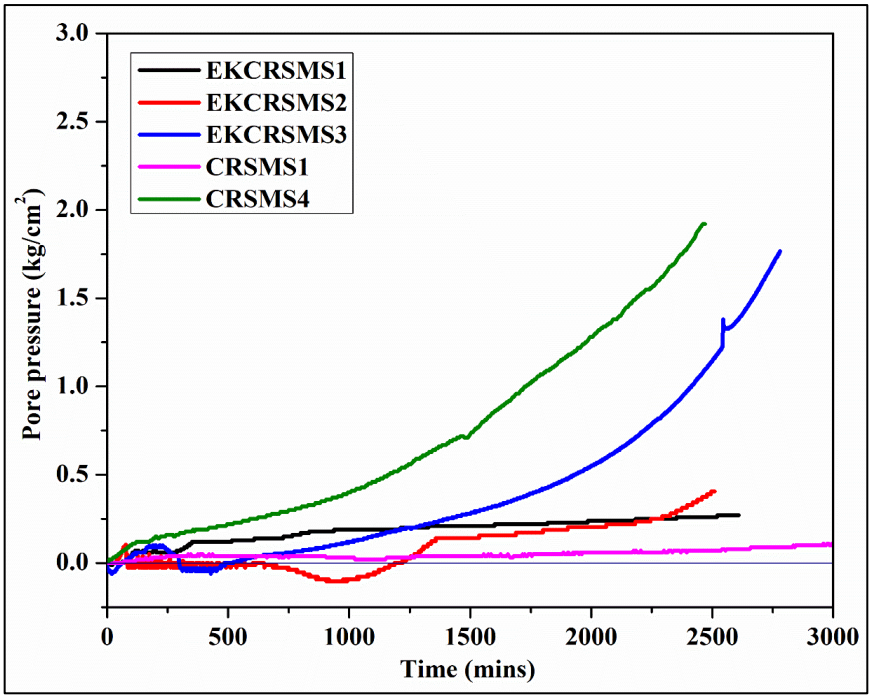

(a)

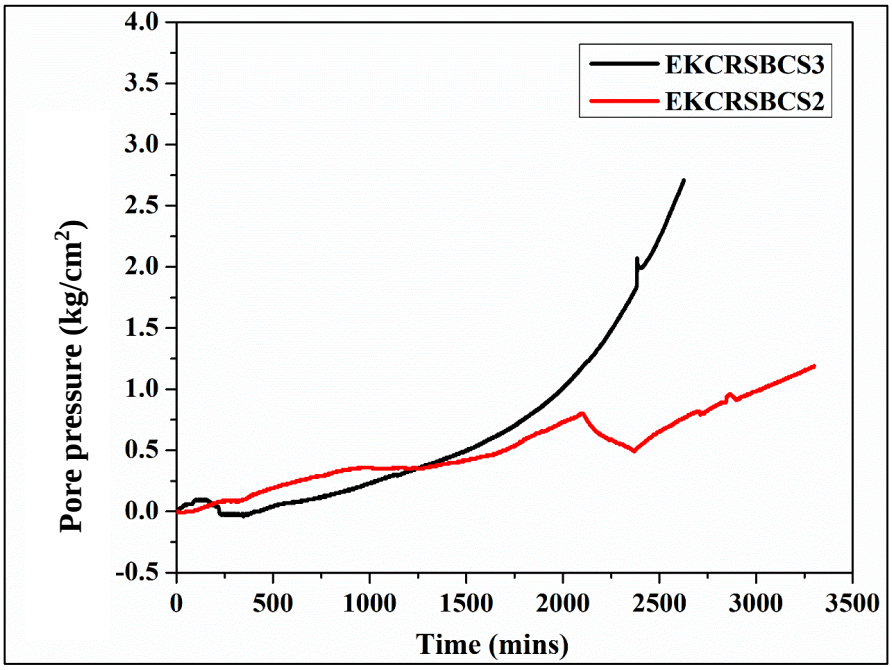

(b)

Figure 6.4 Pore pressure variation with time for different loading conditions for (a) marine soil and (b) black cotton soil

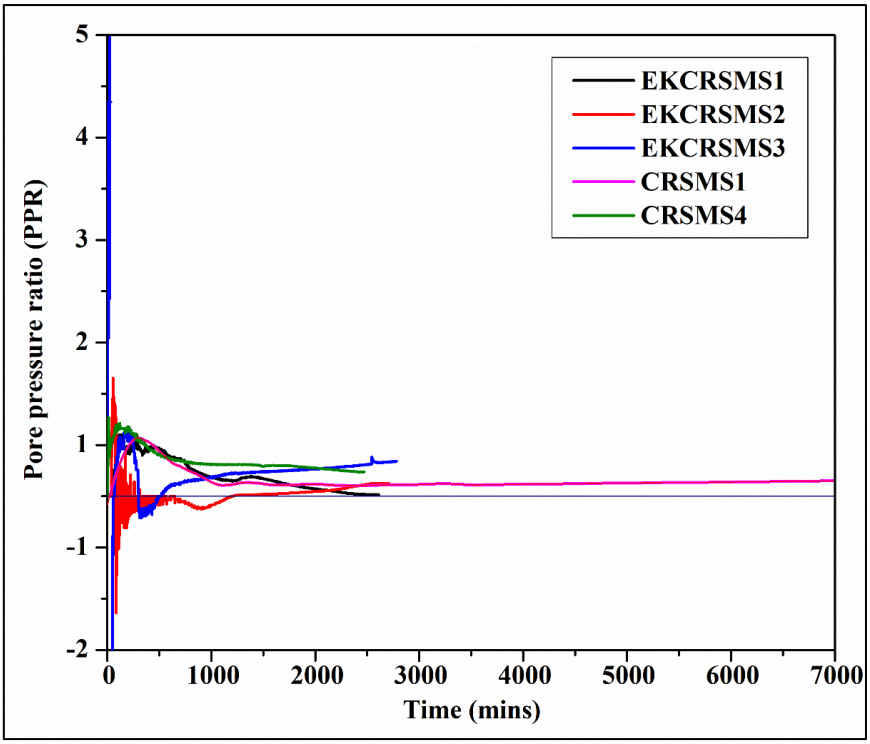

(a)

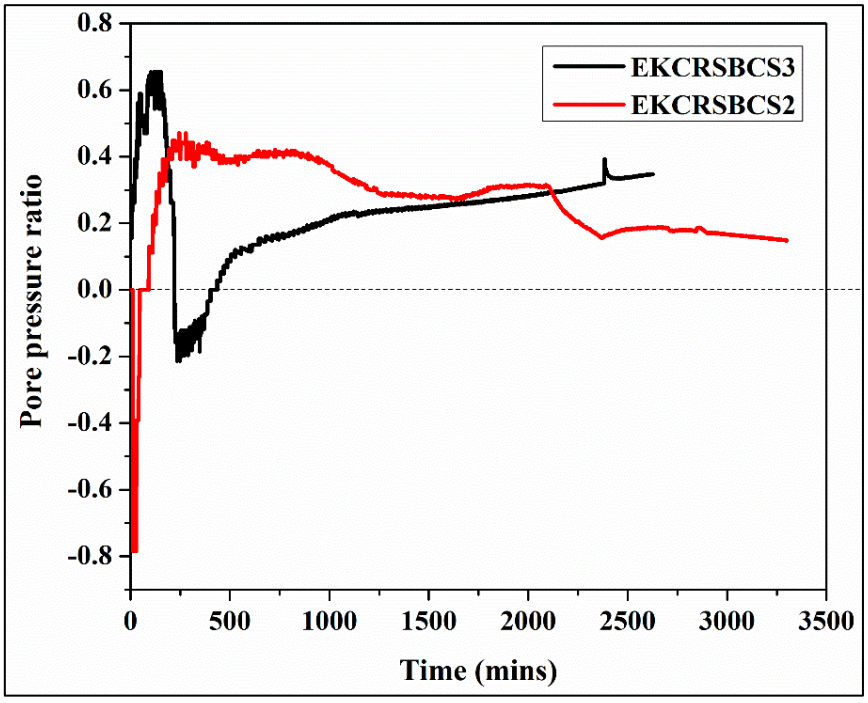

(b)

Figure 6.5 Pore pressure ratio (PPR) variation with time for different loading conditions for (a) marine soil and (b) black cotton soil

6.2.5 Applied voltage effect vs time

Figure 6.6 (a), (b), (c) and (d) illustrates the variation of voltage with time for different EKCL and EKCRS loading conditions for marine soil and black cotton soil. Voltage is an additional parameter that was obtained during the coupled electro-mechanical loading cases in which the electric gradient plays an important role throughout the test. In both loading conditions, the voltage obtained at mid-level of the soil sample was continuously monitored and recorded through the voltage sensor attached to the DAQ. This is dependent on the type of load. In EKCL, the voltage appears to be constant within the range, whereas, for EKCRS the voltage is dependent on the pore pressure dissipation trend. It is noticed that a significant loss of voltage occurred for the applied voltage on soil specimen which is supported by results reported in research (Lo et al.,1991; Jeyakanthan et al., 2011; Ukleja, 2020). The voltage loss that occurred in the vicinity of the anode was found to be less than that at the cathode (Wu et al., 2015; Huey, 2016).). In the case of EKCL loading, this loss in voltage results from the precipitation of metal hydroxides near the cathode and the desorption of metal ions at the anode (Lin Zhang et al., 2018; Yeng et al., 2019). The efficiency factor increased with an increase in applied voltage. A similar observation was made by other researchers (Jeyakanthan et al., 2011). The results indicate that an increase in voltage gradient improves the effective voltage with reference to the output voltage during the early stage of the electrokinetic process. However, from a long-term perspective, an increase in the voltage gradient alone is not useful for increasing the effective voltage to the output voltage.

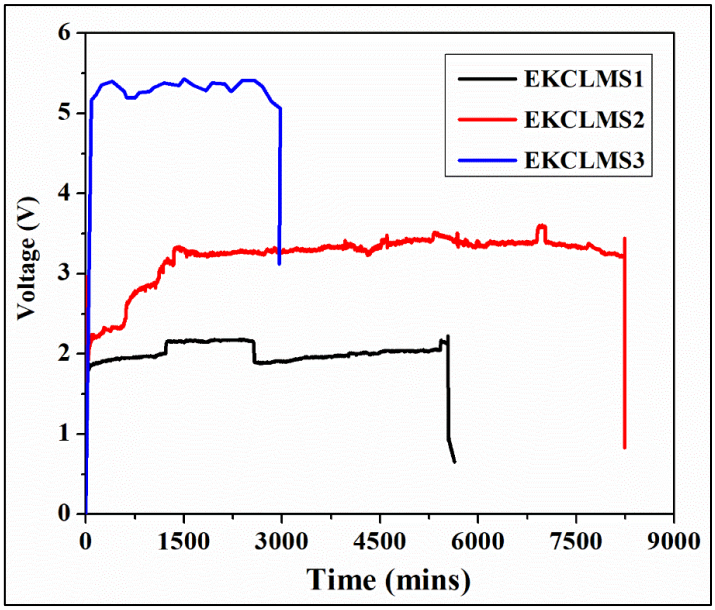
EKCLMS1
EKCLMS2
EKCLMS3
Voltage (V)
Time (mins)
0
1
2
3
4
5
6
0
1500
3000
4500
6000
7500
9000

(a)

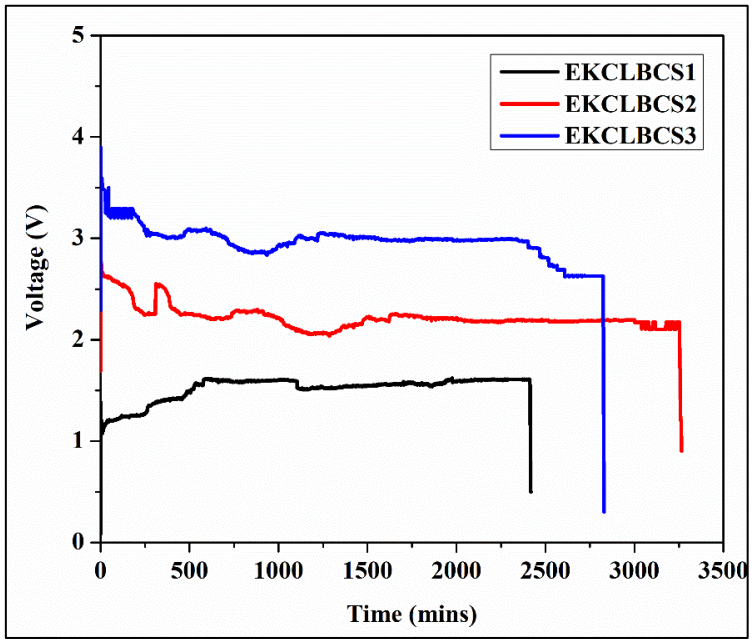
EKCLBCS1
EKCLBCS2
EKCLBCS3
Voltage (V)
Time (mins)
0
1
2
3
4
5
0
500
1000
1500
2000
2500
3000
3500

(b)

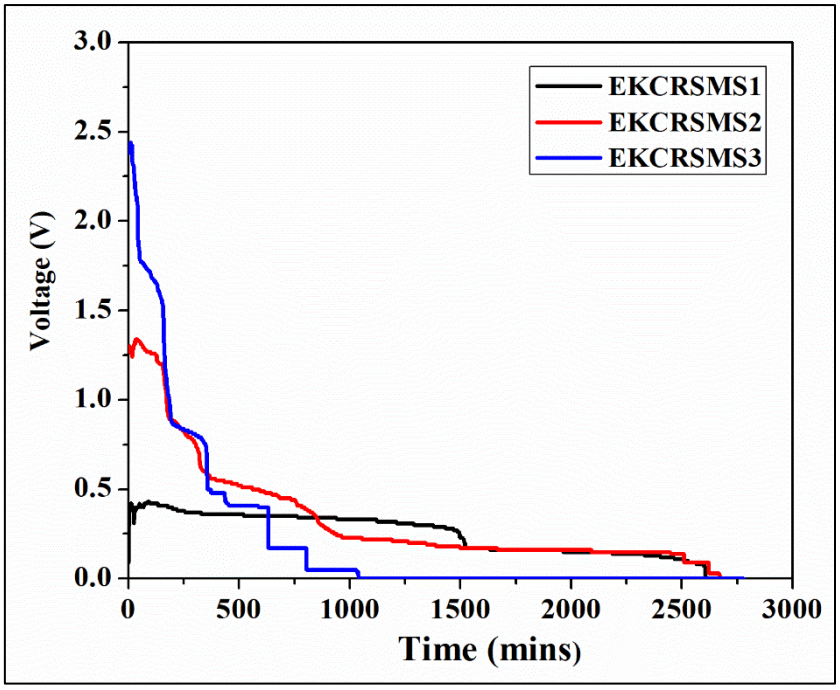

(c)

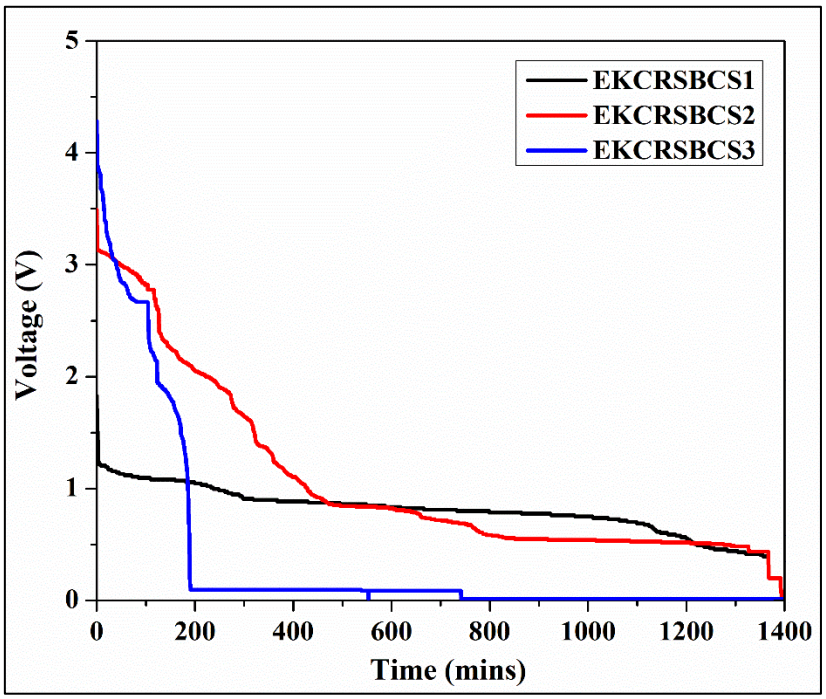

(d)

Figure 6.6 Voltage variation with time (i) EKCL loading for (a) Marine soil and (b) Black cotton soil; (ii) EKCRS loading for (c) Marine soil and (d) Black cotton soil

6.2.6 Current obtained vs time

Current is also an additional parameter monitored throughout the test for different electrokinetic coupled mechanical loading, and the variation of current with time is

depicted in Figure 6.7 (a) and (b). It is observed that the drop in current was rapid in the initial phase and reaches a stable value in the EKCL loading condition. A similar variation of current was reported by several researchers (Lo et al., 1991; Jeyakanthan et al., 2011); Wu et al., 2015). The drop-off in current with time is due to the electrochemical changes leading to an increased rate in the gas bubble formation with time. It increased the resistance between the anode and cathode, resulting in reduced ion mobility, current intensity and consolidation efficiency (Wu et al., 2015; Gargano et al., 2019). Initially, as the voltage gradient is applied, acidic and basic fronts developed at the anode and cathode which causes heterogeneous ion concentration in the soil-water system. This heterogeneous ion concentration reduces the electrical conductivity of soils and releases the H^+ ions in the expelled pore fluid near the anode (Jeyakanthan et al., 2011; Kollannur and Arnepalli, 2019)

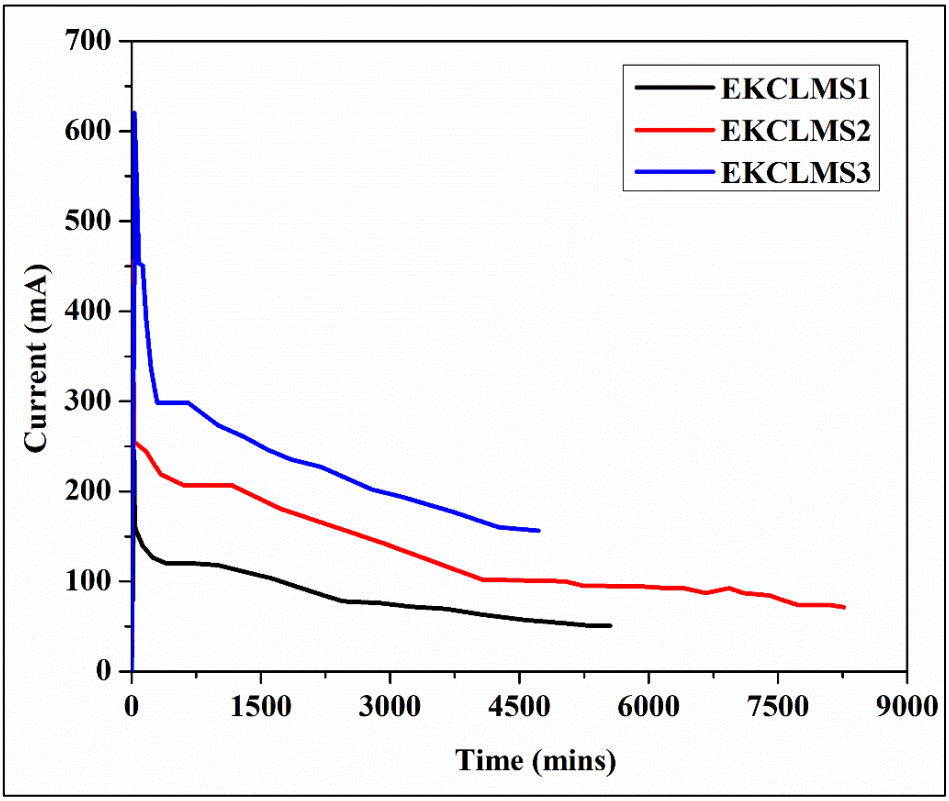

(a)

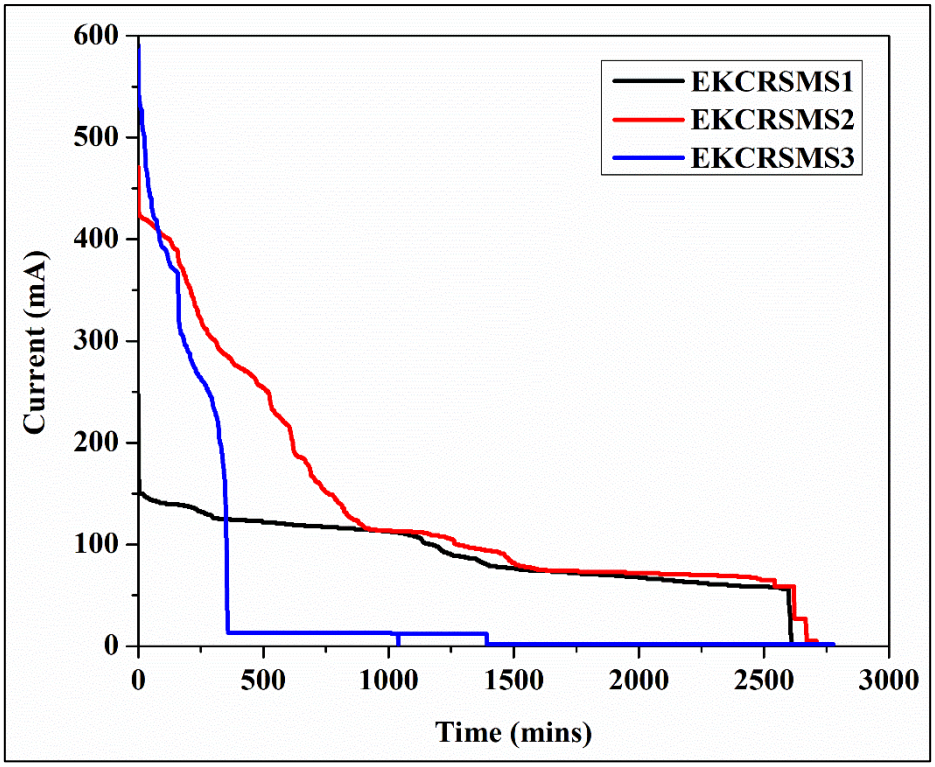
EKCRSMS1
EKCRSMS2
EKCRSMS3
Current (mA)
Time (mins)
0
100
200
300
400
500
600
0
500
1000
1500
2000
2500
3000

(b)

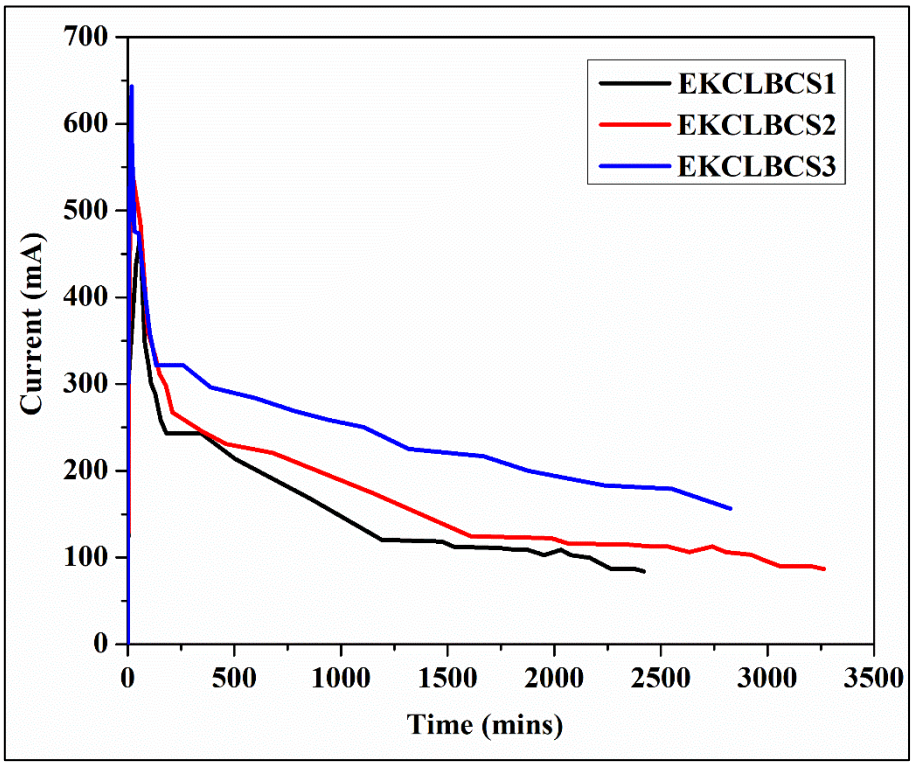
EKCLBCS1
EKCLBCS2
EKCLBCS3
Current (mA)
Time (mins)
0
100
200
300
400
500
600
700
0
500
1000
1500
2000
2500
3000
3500

(c)

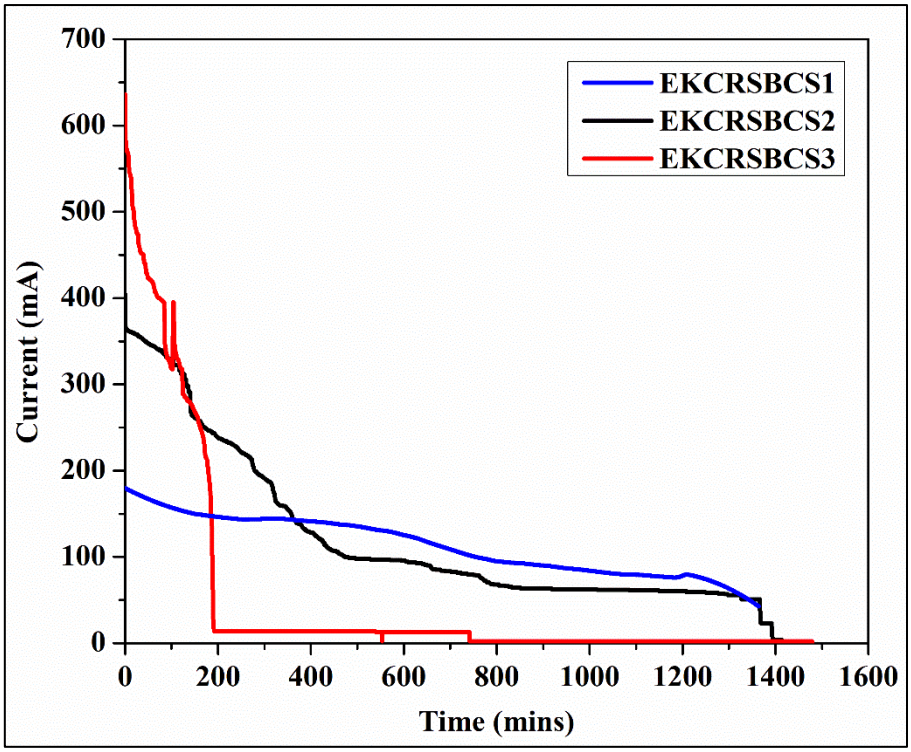

(d)

Figure 6.7 Current variation with time (i) EKCL loading for (a) Marine soil and (b) Black cotton soil; (ii) EKCRS loading for (c) Marine soil and (d) Black cotton soil

6.2.7 pH vs sample location

pH is also an additional parameter that needs to be considered during the electrochemical process, as OH^- ion (alkaline agent) is transferred which leads to the H^+ ion (acidic agent) movement from the anode surface to the cathode to neutralize and obstruct OH^- ion movement (Zhang et al., 2018; Korolev and Nesterov, 2019; Kherad et al., 2020). In clay particles, the H^+ ion is adsorbed by negatively charged clay particles due to its buffering capacity. This results in an increased pH value from the anode (bottom) to the cathode (top) as shown in Figure 6.8. In addition, with an increase in voltage, the movement of H^+ and OH^- ions will increase resulting in a higher variation of pH value. During the process, the pH of the soil in the vicinity of the anode decreases and the cathode increases (Ye, 2016; Sadeghian et al., 2022). Similar observations for pH value were also presented (Jeyakanthan et al., 2011; Malekzadeh and Sivakugan, 2017; Lin Zhang et al., 2018; Xue

et al., 2020). The chemical reactions involved in the pH value trend due to the electrolysis process breaks down the water molecule as follows (Jeyakanthan et al., 2011)

$$2H_2O = 4H^+ + O_2 \uparrow + 4e^- \text{ (anode)} \quad \text{(Eq. 6.1)}$$

$$4H_2O = 4OH^- + 2H_2 \uparrow - 4e^- \text{ (cathode)} \quad \text{(Eq. 6.2)}$$

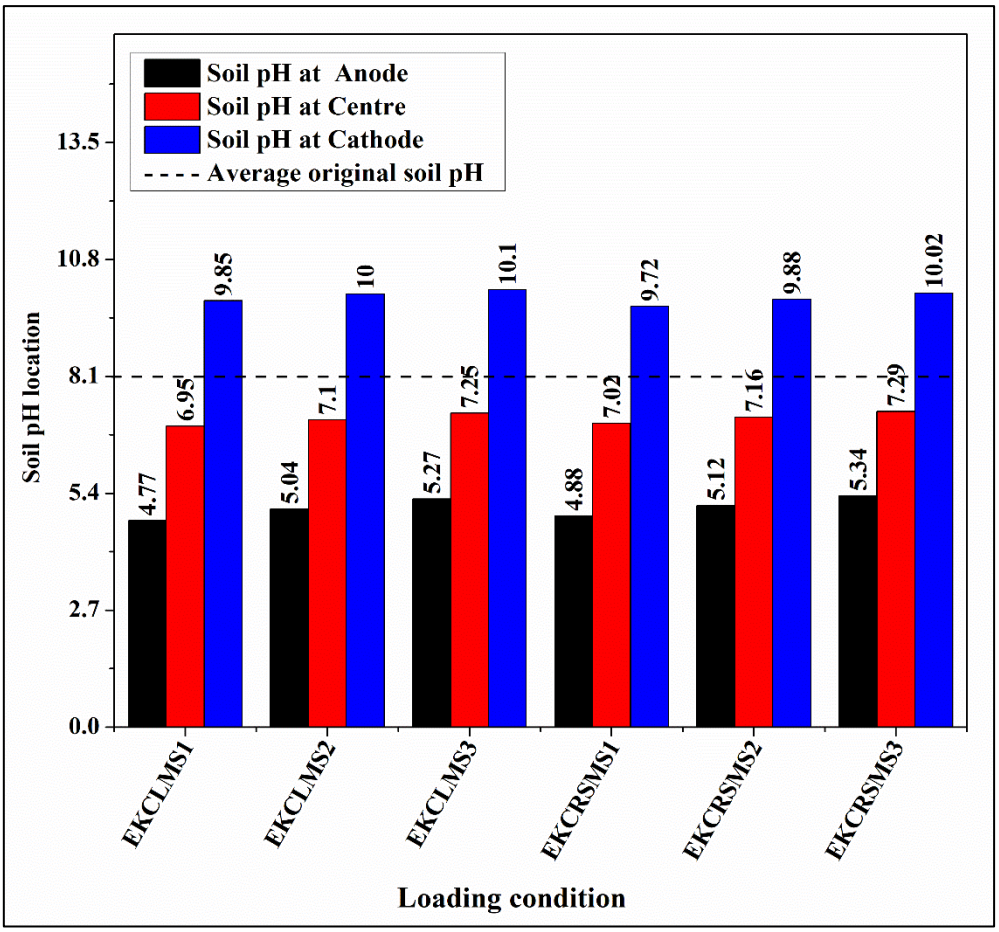

(a.)

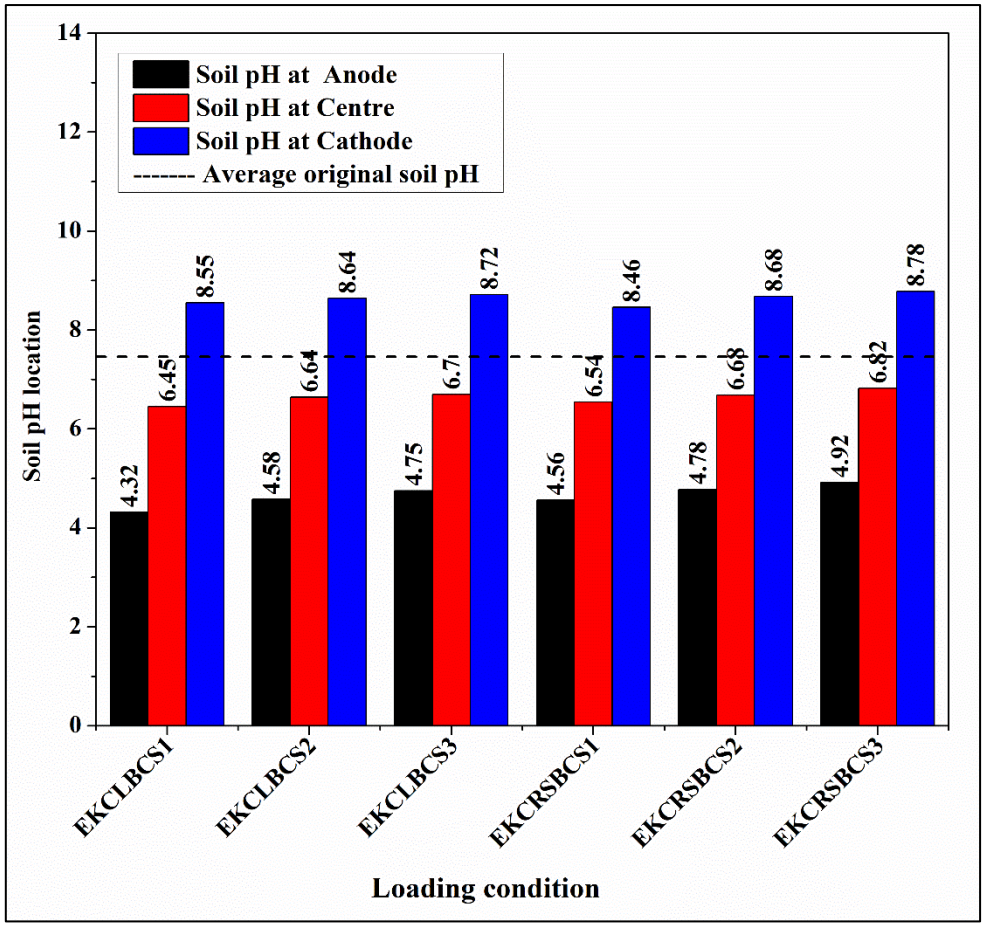

(b.)

Figure 6.8 Soil pH vs different loading conditions for coupled electro-mechanical loading for (a) Marine soil and (b) Black cotton soil

6.2.8 Moisture Content of Soil

The moisture content of the soil samples for pre- and post-EK consolidation tests subjected to various loading conditions was found and reported in Figure 6.9. In the case of EK consolidation, it was observed that the fluid movement resulting from the electrochemical changes and complex mechanism leads to a non-uniform moisture content variation across the soil samples. Huey (2016) also reported a similar finding. The reason behind the phenomenon is the movement of positively charged particles towards the cathode (negative front), while negatively charged particles toward the anode (positive front). This is due to the accelerated expulsion of interstitial water under an applied electric gradient which ultimately consolidates the soil. On the other hand, a uniform distribution of moisture content was observed only in mechanical loading.

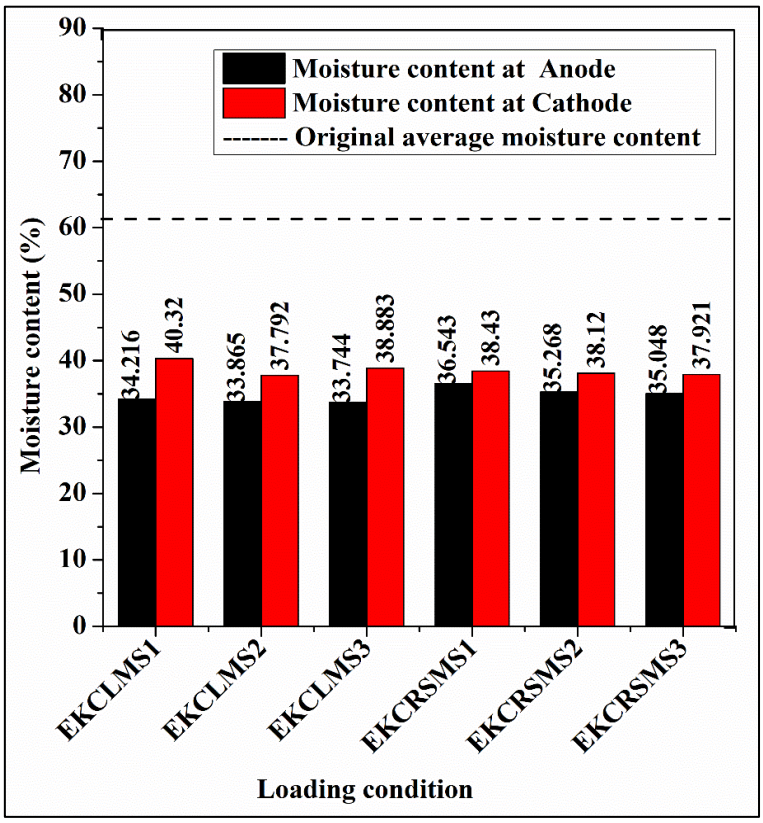
Moisture content at Anode
Moisture content at Cathode
------- Original average moisture content
Moisture content (%)
0
10
20
30
40
50
60
70
80
90
34.216
40.32
33.865
37.792
33.744
38.883
36.543
38.43
35.268
38.12
35.048
37.921
EKCLMS1
EKCLMS2
EKCLMS3
EKCRSMS1
EKCRSMS2
EKCRSMS3
Loading condition

(a)

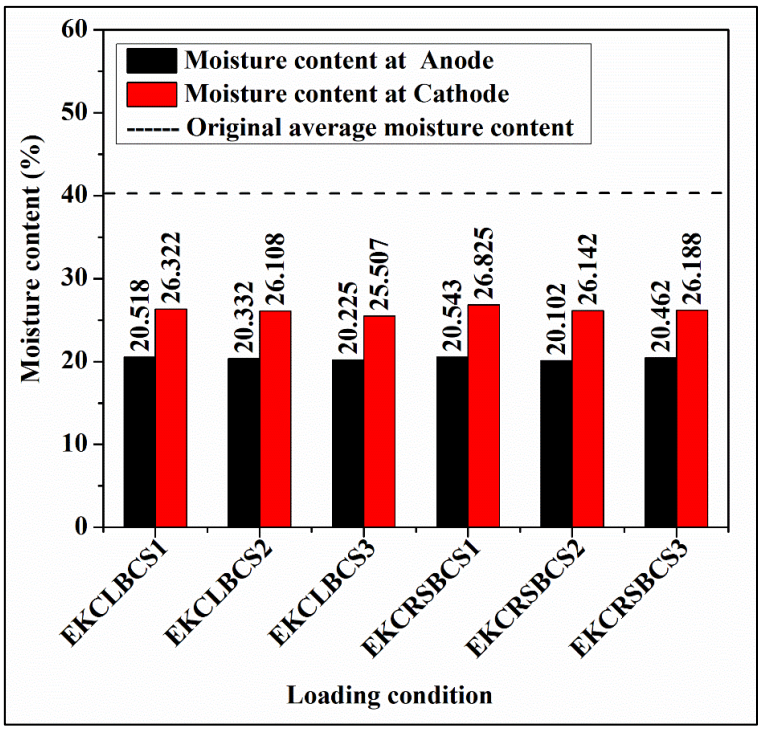
Moisture content at Anode
Moisture content at Cathode
------ Original average moisture content
Moisture content (%)
0
10
20
30
40
50
60
20.518
26.322
20.332
26.108
20.225
25.507
20.543
26.825
20.102
26.142
20.462
26.188
EKCLBCS1
EKCLBCS2
EKCLBCS3
EKCRSBCS1
EKCRSBCS2
EKCRSBCS3
Loading condition

(b)

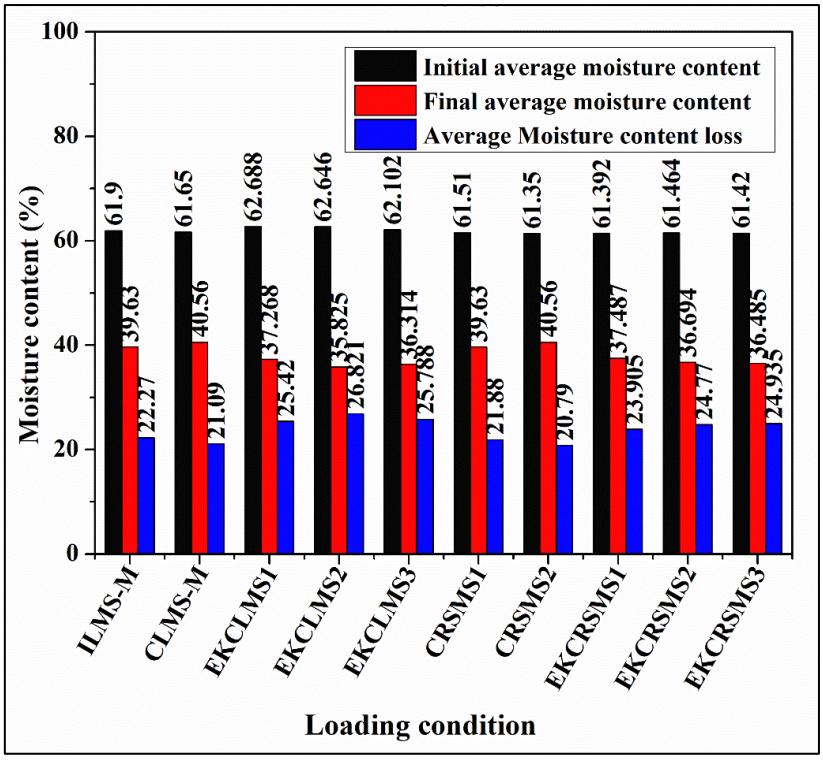

(c)

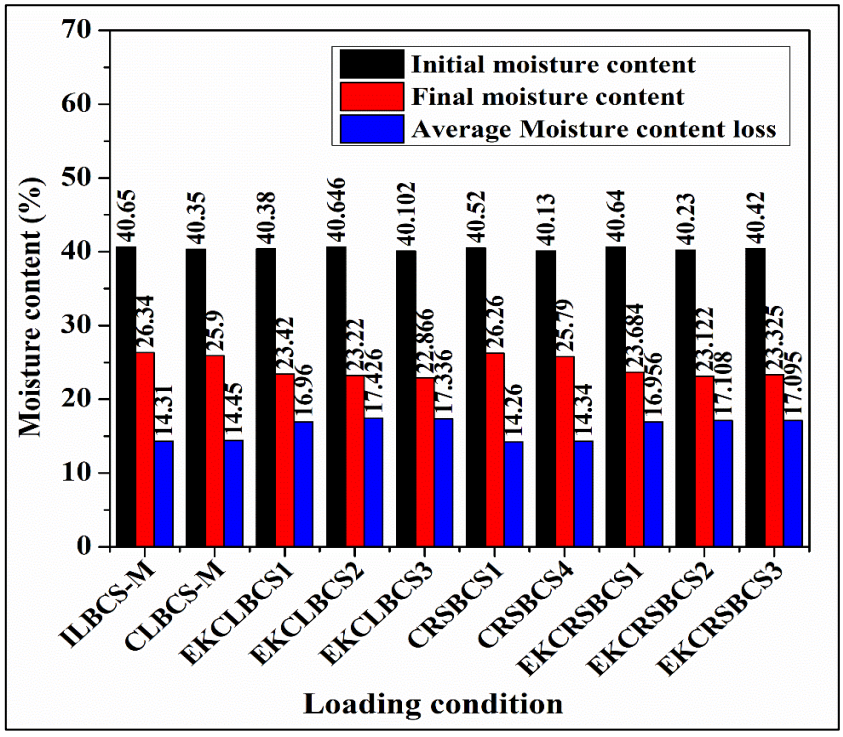

(d)

Figure 6.9 (i) Coupled electro-mechanical loading moisture conditions at anode, cathode and average moisture content (a) Marine soil and (b) Black cotton soil; (ii) Coupled electro-mechanical loading conditions at the initial, final and average moisture content (c.) Marine soil and (d) Black cotton soil

6.3 Microstructure Study

6.3.1 Scanning electron microscopy (SEM)

The microfabric/particle arrangement of soil can be investigated with representative scanning electron microscopy (SEM) of the dried soil before and after the electro-osmosis process (Wu et al., 2016). Soil properties and characteristics depend on the intermediate microstructure of dispersed and flocculated soil (Sachan et al., 2012); Moayedi et al., 2014; Korolev and Nesterov, 2019; Gargano et al., 2020). The compressibility and consolidation characteristics are the results of clay matrices, interstitial pore spaces, diffuse double layer (DDL), and soil particle aggregation (Kaniraj, 2014; Kollannur and Arnepalli, 2019). These physical characteristics can be recognized with the SEM image for all microstructure features like particle arrangements, particle assemblage and pore spaces (Gargano et al., 2020)

Figure 6.10 shows the induced microfabric changes within the inter-electrode space for coupled loading EKCLMS2 when compared with the original soil sample. An alteration in micro-fabric can be seen in the image. The microfabric size increased due to the contraction of the DDL envelope and bonding with the negatively charged particle. Another main characteristic is the redistribution of pore size visible within the treated soils. At the anode front, the size of micro aggregates decreased sharply in a highly acidic medium due to the dissolution of clay particles but at the cathode front, micro-aggregates size increased. Electro-osmosis caused the formation of anisotropic large pores (macropores) within the cathode and anode zone. Similar findings were also reported by (Korolev and Nesterov, 2019)y (Korolev and Nesterov, 2019).

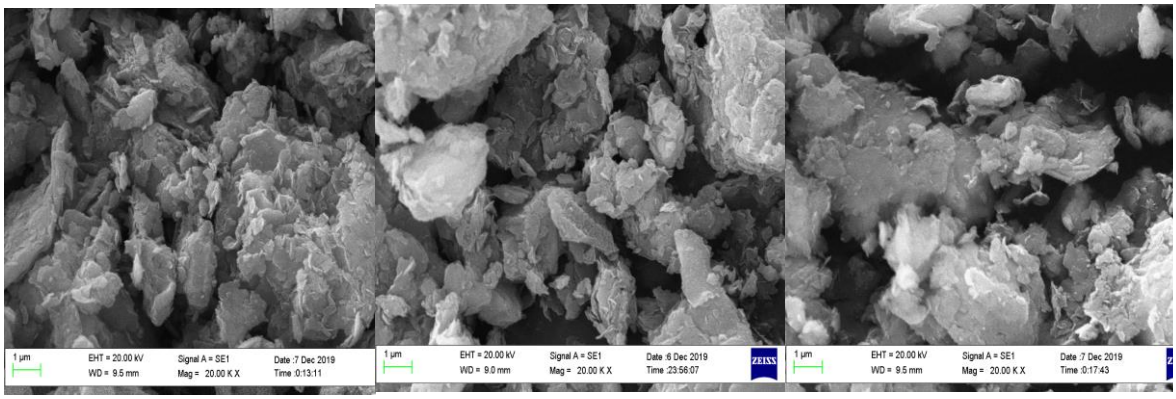

At anode front **Original soil** **At cathode front**

Figure 6.10 SEM images of marine soil at anode, original and cathode section

6.3.2. Images Before and After Consolidation Test

The EK loading tests conducted on reconstituted Marine soil samples resulted in additional pore-water expulsion, leading to an increased volume reduction. The interpretation of data obtained from EK loading tests such as deformation, void ratio, and water content after the test validates the success of the EK consolidation technique when compared to conventional tests. Figure 6.11 displays a few photographs related to the coupled experiment, providing a better understanding of the chemical and physical changes taking place in soil and electrodes after the electrochemical action. Figure 6.11(a) shows the formation of gas bubbles during the initial stages of the consolidation test carried out with voltage coupled loading, and the gas formation is directly proportional to the voltage applied. Figure 6.11(b) illustrates the final stage of the voltage coupled consolidation process. Heavy deposition of electrode precipitation was observed on the loading pad, and precipitation occurred because of the electrokinetic phenomenon at the cathode front, which increased the resistivity of the soil. The variation of the anode and cathode electrodes after the completion of the test is depicted in Figure 6.11(c) and (d), respectively. This can be attributed to the oxidation and reduction of copper with a deteriorated condition of the copper electrode (anode) after completion of the test due to the complex phenomenon

involved with the electrokinetic coupled test, and oxidation of copper electrode and generation of oxygen gas and for Cathode reduction of the copper electrode and generation hydrogen gas. A higher loss of moisture content in soil at the anode in comparison to the cathode was observed, and the anode and cathode sides of the soil are shown in Figure 6.11(e) and (f), respectively. Lastly, Figure 6.11(g) presents the side view of the sample after removing it from the consolidation ring.

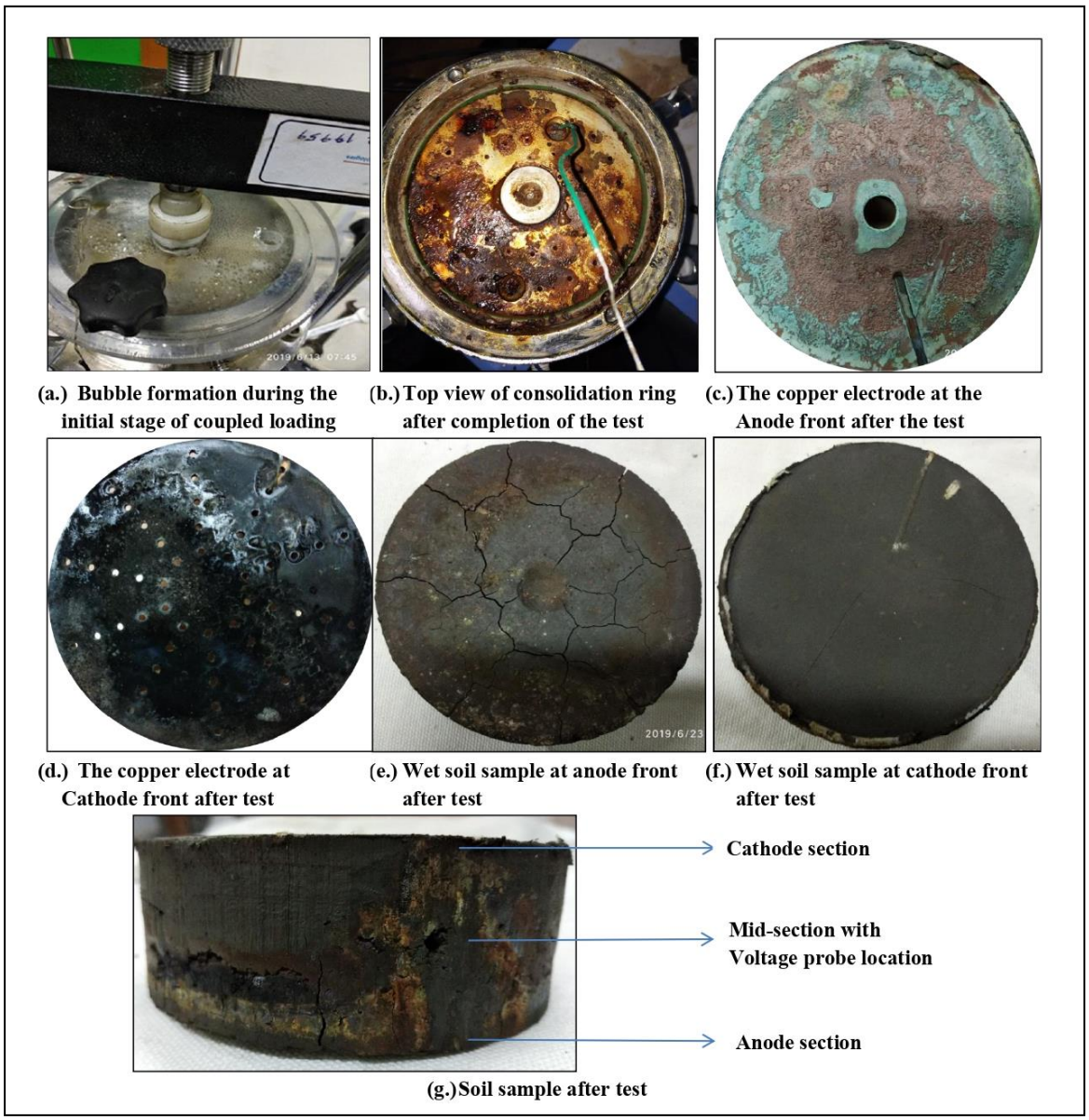

Figure 6. 11 Photographs of soil and electrodes before and after the voltage-coupled loading

6.4. Summary

The present chapter aimed to test the results of EKCL and EKCRS using a modified consolidation system for performing coupled electro-mechanical loading effects. This system was designed with the capability to expel gases generated from complex electro-mechanical phenomenon at the anode and cathode ends. The system performed satisfactorily during consolidation tests marine and black cotton soil samples. The experimental data were analysed, compared, and validated with conventional consolidation systems effectively.